scientific reports

Check for updates

OPEN

Robinin attenuates cardiac oxidative stress-induced endoplasmic reticulum-dependent apoptosis through AKT/GSK3β pathway

N. Abhirami[1], V. A. Aswathy[3] & Janeesh Plakkal Ayyappan[1,2]✉

Myocardial injury is a pathological condition often resulting from excessive β-adrenergic stimulation, such as that induced by isoproterenol (ISO), a β-adrenergic agonist that increases reactive oxygen species (ROS) production, leading to endoplasmic reticulum (ER) stress, apoptosis, and impaired survival signaling. This study investigated Robinin's (Rob) ability to mitigate ISO-induced myocardial damage in H9c2 cardiomyocytes and male Sprague-Dawley rats. ISO-induced damage was assessed through histology, oxidant/antioxidant assays, cardiac marker enzyme assays, and molecular analyses, including PCR and Western blotting. Rob treatment significantly reduced ISO-induced ROS generation and apoptosis, while preserving cell morphology and survival. Rob also modulated ER stress and apoptosis-related proteins, restoring cardiomyocyte function in a dose-dependent manner. Western blot analysis confirmed Rob's inhibition of ER stress-mediated apoptosis in both *in vitro* and *in vivo* models. These findings suggest that Rob exerts potent cardioprotective effects by reducing oxidative stress, modulating ER stress, and inhibiting apoptosis. Its ability to restore ER function and cardiomyocyte viability highlights its potential as a therapeutic agent for ISO-induced myocardial damage.

Keywords Cardio protection, ER stress, Rob, Myocardial infarction, Therapeutic agent

Abbreviations

CVD	Cardiovascular Disease
MI	Myocardial Infarction
ISO	Isoproterenol
ERS	Endoplasmic Reticulum Stress
Met	Metoprolol Succinate
RT-PCR	Real-Time Polymerase Chain Reaction
α-MHC	Alpha Myosin Heavy Chain
β-MHC	Beta Myosin Heavy Chain
SOD	Superoxide Dismutase
CAT	Catalase
ROS	Reactive Oxygen Species
FACS	Fluorescence-Activated Cell Sorting
AO/EB	Acridine Orange/Ethidium Bromide
FITC	Fluorescein Isothiocyanate
PI	Propidium Iodide
CK-MB	Creatine Kinase-MB
LDH	Lactate Dehydrogenase

[1]Translational Nanomedicine and Lifestyle Disease Research Laboratory, Department of Biochemistry, University of Kerala, Kariavattom campus, Thiruvananthapuram 695034, Kerala, India. [2]Centre for Advanced Cancer Research, Department of Biochemistry, University of Kerala, Kariavattom campus, Thiruvananthapuram 695034, Kerala, India. [3]Department of Anatomy, P K Das Institute of Medical Sciences, Vaniyamkulam, Ottapalam, Palakkad 679522, Kerala, India. ✉email: janeeshbiochemistry@keralauniversity.ac.in

MDA	Malondialdehyde
SGOT	Serum Glutamic Oxaloacetic Transaminase
TTC	Triphenyl Tetrazolium Chloride
CHOP	C/EBP Homologous Protein
Bip	Binding Immunoglobulin Protein
ATF 6	Activating Transcription Factor 6
PDI	Protein Disulfide Isomerase
Bax	Bcl-2 Associated X Protein
Bcl-2	B-Cell Lymphoma 2
AKT	Protein Kinase B
GSK 3-β	Glycogen Synthase Kinase 3 Beta
ERK1/2	Extracellular Signal-Regulated Kinase 1/2

Cardiovascular disease (CVD) encompasses a wide variety of disorders affecting the heart and blood vessels, such as hypertension, heart failure, coronary artery disease, and stroke. When combined, these medical disorders are among the world's most serious health challenges, affecting a significant number of people each year[1]. Myocardial infarction (MI), sometimes known as a heart attack, is a specific symptom of CVD that is intrinsically linked to a broader set of CVD-related conditions.

Long-term ischaemia is produced by an imbalance in oxygen supply and demand, which leads to MI. This causes necrosis of the heart muscle and a reduction in contractile ability. According to recent studies, oxidative stress, inflammation, and apoptosis all play essential roles in the pathophysiology and progression of MI. Experimental models are essential for understanding the pathophysiology of MI and discovering novel therapeutic targets for intervention. Isoproterenol (ISO), a non-selective beta-adrenergic agonist, has gained popularity because of its ability to cause cardiac damage both *in vitro* and *in vivo*. ISO-induced MI models provide various benefits, including the ability to replicate certain aspects of human MI pathophysiology, as well as control and repeatability[2].

The fundamental goal of modern MI therapy approaches is the quick revascularisation of the affected heart muscle. This can be performed by surgery and pharmacological treatments such as anticoagulants, antiplatelet medications, and fibrinolytic therapy. Long-term therapy for MI patients includes nitrates, beta blockers, lipid-lowering drugs, and angiotensin-converting enzyme (ACE) inhibitors[3]. Because of their limited effectiveness, these long-term treatments are not appropriate for many MI patients. Novel therapeutic strategies that might enhance the regeneration and repair of injured cardiac tissue are thus urgently needed. One exciting area of research is the use of phytochemicals, which are bioactive compounds obtained from plants that have the potential to improve cardiovascular health. These chemical compounds have the potential to be cardioprotective, anti-inflammatory, and antioxidant, making them intriguing options for new treatment techniques of MI.

Robinin (Rob) is made up of the flavonoid aglycone kaempferol connected to three sugar moieties: two glucose molecules and one rhamnose. Rob is used to treat CVDs because of its ability to improve endothelial function, reduce oxidative stress, and inhibit platelet aggregation. Eom et al. discovered that Rob inhibited the synthesis of cyclooxygenase-2, interleukin-6, tumour necrosis factor-α, and inducible nitric oxide synthases. Rob alters the TLR-NF-κB signalling pathway by inhibiting NF-κB p65 translocation and blocking oxidised low-density lipoprotein (ox-LDL), which increases the development of TLR2 and TLR4[4].

Metoprolol succinate (Met) serves as a positive control in this study since it has been found to lower heart rate and myocardial oxygen demand. Met, a β1-selective adrenoceptor blocking drug lowers blood pressure by decreasing heart rate and muscle contraction force. Met's capacity to control these haemodynamic parameters and increase cardiac efficiency makes it a recommended therapy for MI[5,6].

ISO-induced stress connects the protein kinase B (AKT), apoptotic, and Endoplasmic Reticulum Stress (ERS) pathways. These interactions are complicated and crucial for understanding how cells respond to stress, notably in the cardiopulmonary system and blood vessels[7]. Severe or unresolved ERS may impede AKT signalling, perhaps by activating CHOP, a pro-apoptotic transcription factor activated under severe ER stress[8].

In the present research, we aimed to better understand the processes causing ISO-induced MI by simulating myocardial injury in a controlled environment and investigating cellular and signaling responses such as oxidative stress, apoptosis, and alterations in gene expression patterns associated with MI. We used multiple approaches to acquire insights into the cellular and molecular pathways involved in ISO-mediated cardiac injury and examine possible treatment options.

Materials and methods

Materials

Sigma (Sigma-Aldrich, USA) supplied Rob, isoproterenol, dimethyl sulfoxide (DMSO), Metoprolol succinate, Triphenyl tetrazolium chloride (TTC), Hematoxylin, Eosin and dichlorodihydrofluorescein diacetate (DCFH-DA). Himedia (Maharashtra, India) supplied the antibiotic penicillin-streptomycin, trypsin (0.25%), and MTT [3-(4,5-dimethylthiazol-2yl)−2,5-diphenyltetrazoliumbromide]. Gibco (Gibco, Grand Island, NY, USA) supplied DMEM, PBS, and foetal bovine serum. H9c2 cell line was received from ATCC (Manassas, Virginia), and Trizol reagent was obtained from SRL (Mumbai, India). Assay kits were bought from Origin Diagnostics and Research in Kerala, India. Thermo Fisher Scientific Inc. (United States) supplied the fluorescent dyes, Pierce BCA Protein Assay Kit, GeneJET RNA purification kit, Power SYBR® Green Master Mix, and Verso cDNA Synthesis Kit. APJ Scientific Solutions (Trivandrum, India) synthesised the forward and reverse real-time PCR primers. Antibodies were bought from Cell Signalling Technology (Massachusetts, USA). All of the compounds used were analytic grade.

Experimental design

24 male 6 week old Sprague Dawley rats weighing between 150 and 180 g were acquired from the Mannuthy College of Veterinary and Animal Sciences. They were housed in a specific pathogen-free, temperature and humidity-controlled environment (25 ± 2 °C, 50 ± 5% humidity) with a standard 12 h Light/12 h Dark cycle at University of Kerala's Department of Biochemistry. During the course of the trial, rats were given an unlimited supply of standard diet and water ad libitum.

Ethical statement The study was approved by University of Kerala Institutional Animal Ethical Committee (IAEC sanction no. IAEC 2-KU-01/2023-BCH-JA (08)), in accordance with the guidelines of the Committee for the Control and Supervision of Experiments on Animals (CCSEA), Government of India. All animal experiments were conducted following ARRIVE guidelines, ensuring compliance with current animal welfare regulations. Every effort was made to minimize the number of animals used and their suffering. The number of rats used in each experiment is specified in the corresponding figure legends.

Cardiac H9c2 cell culture

H9c2 cells derived from rat embryonic cardiomyocytes were acquired from ATCC, Manassas and maintained in high glucose DMEM supplemented with 10% (v/v) heat-inactivated FBS, 100 µg/mL penicillin-streptomycin. H9c2 cardiomyoblasts were differentiated using the methods previously reported[9,10]. In summary, H9c2 cells were treated with retinoic acid (10 nM) every day for 6–7 days in DMEM with 1% FBS.

Confirmation of differentiated cardiomyocytes

H9C2 differentiation was investigated by monitoring morphological changes, performing gene expression analysis with qRT-PCR, protein expression with western blotting, and stimulating differentiated cells with ISO.

In vitro experimental design

Cardiomyocytes were cultured in 96-well plates at a density of 2×10^5 cells/well and differentiated as previously described. After reaching 80% confluence, the cells were divided into five groups

Cells cultured in medium without drugs and used as a control

Cells cultured in medium containing 50 µg/ml Rob and named as Rob group

Cells cultured in medium containing 50 µg/ml Rob and 100 µM of ISO and named as Rob + ISO group

Cells cultured in medium containing 50 µM Met and 100 µM of ISO and named as Met + ISO group

The dose of ISO was determined by reviewing previous publications[11]. The following studies were carried out on the cells after they had been grown for 24 h.

Protective effect of Rob

H9c2 cardiomyocytes were cultured in a 96-well plate and treated with 50 µg/ml Rob and Met for 24 h. The cultures were then treated with 100 µM ISO for 24 h. The MTT test was used to determine cell viability. The absorbance was measured at 570 nm with a microplate reader (BioTek Instruments Inc., Winooski, USA). The morphological changes in the cells were examined and documented using an inverted microscope (EVOS XL Core).

Detection of intracellular reactive oxygen species (ROS)

$DCFH_2$-DA, a cell-permeable fluorescent probe, was utilised to quantify intracellular ROS. H9c2 cells were pre-treated with Rob and Met, and then exposed to ISO for 24 h. The samples were incubated with 10 µM $DCFH_2$-DA for 20 min at 37 °C in the dark. After incubation, cells were gently rinsed with PBS thrice and subsequently fixed with 4% paraformaldehyde for 10 min at room temperature. Following fixation, nuclei were counterstained with DAPI for 5 min to visualize nuclear morphology. Images were captured using a microscope (ZOE Fluorescent Cell Imager, BioRad) at 100 x magnifications with a filter of emission wavelengths 510–550 nm and excitation wavelengths 470–490 nm and DAPI.

Intracellular ROS levels were measured by Fluorescence-activated cell sorting. After treatment, the cells were then trypsinised, collected, and washed three times with PBS before centrifugation at 1000 g for two minutes. The cell pellets were resuspended in 1 ml of cold PBS and analysed using a BD FACS Aria III (BD FACSDiva version 7.0). The results were reported as the percentage of fluorescence intensity relative to the control.

Acridine orange/ethidium bromide (AO/EtBr) double staining

Rob's protective effect against ISO-induced necrosis and apoptosis was assessed using a fluorescent double-staining technique with AO/EB. 5×10^3 cells were seeded in a 12-well plate and differentiated as previously described. The groups were subsequently treated according to the procedures mentioned above. After treatment, adherent cells were washed twice with PBS (pH 7.4). Each group was re-suspended with a 1 ml working solution containing a 1:1 solution of AO (100 µg/ml)/EB (100 µg/ml) and incubated for 30 min at 37 °C in the dark. The unbounded stain was then rinsed thoroughly with PBS. A fluorescent microscope (ZOE Fluorescent Cell Imager, BioRad) was used to differentiate live and dead cells in each well.

Determination of cellular apoptosis

Annexin V detects early and late apoptosis in cells by binding to the phosphatidylserine (PS) on the cell's outer leaflet. 2×10^5 cells were seeded in a six-well plate and treated as mentioned above. The cells were rinsed with 1X binding buffer and stained with Annexin V (5 µL) and propidium iodide (10 µL) as instructed by the Apoptosis Detection Kit (Invitrogen, USA). The apoptotic cells of each group were quantified through BD FACS Aria III (BD FACSDiva version 7.0). Early apoptotic cells were identified as Annexin V^+/PI^-, while late apoptotic or necrotic cells were Annexin V^+/PI^+.

Experimental animal models of ISO-induced myocardial injury

The animals were randomly divided into 4 groups of 6 animals each and the experimental period was 14 days.

Group I (Control group): Rats were injected with 100 µl normal saline for 14 days intravenously.

Group II (ISO group): Rats were injected with 100 µl normal saline for 14 days intravenously and ISO (85 mg/kg, s.c.) in normal saline on 13th and 14th day at an interval of 24 h.

Group III: (Rob group): Rats were injected with Rob in normal saline (20 mg/kg, i.v) for 14 days intravenously.

Group IV: (Rob + ISO group): Rats were injected with Rob in normal saline (20 mg/kg, i.v) for 14 days intravenously and ISO (85 mg/kg, s.c.) in normal saline on the 13th and 14th days at an interval of 24 h[12].

The rats were euthanized using 5% isoflurane, administered through an induction chamber, followed by cervical dislocation to ensure humane euthanasia.

Estimation of lipid peroxidation products and antioxidants

Heart tissues and H9c2 cells were collected, sonicated, and their protein concentration was measured with a Pierce BCA Protein Assay Kit. The cells were then collected in accordance with the manufacturer's instructions supplied by Origin Diagnostics and Research (Kerala, India) to assess the level of MDA (2202-01), CAT (3303-01), and SOD (3302-01). Each test was conducted in quadruples.

Measurement of myocardial infarct size

MI size was determined using the direct triphenyl tetrazolium chloride (TTC) technique. The process entailed cutting the heart transversely across the left ventricle with a thickness of 2 to 3 mm, then incubating it in a 1% TTC solution in phosphate buffer (pH 7.4) for 30 min at 37 °C. The sections were then preserved using 10% formalin. The infarcted myocardium was pale grey or white, while the non-ischemic myocardium was dyed red.

Pathological changes of myocardial tissue

Heart tissue was extracted and fixed in 4% paraformaldehyde for 24 h, then dried, embedded, and sliced to 5 µm. Routine H&E was done. After sealing, the alterations in myocardial histopathology were examined under an optical microscope (EVOS XL Core).

Myocardial injury determination

Blood samples were collected and centrifuged to obtain serum. Myocardial injury indexes of LDH (6603-01), SGOT (11408005), and creatine kinase (11404001) in serum and LDH in cultural supernatant *in vitro* were determined by a commercial kit purchased from Origin and Agappe Diagnostics Ltd, India.

SYBR green real-time PCR assay for gene expression

Trizol reagent was used to extract total RNA from tissues and cells. Gene expression levels of α-MHC, β-MHC, α-actinin, CHOP, Bip, ATF 6, PDI, Cas 3, Cas 9, BAX, and Bcl-2 were analysed following treatments. The RNA content and purity were estimated using a nanoplate reader and the ratio of absorbance readings at 260 and 280 nm (A260/A280) was taken. The Verso cDNA Synthesis kit was used to reverse transcribe 1 µg of total RNA extracted from each sample into cDNA, as per the manufacturer's instructions. Power SYBR® Green Master Mix was used to create PCRs for each group's real-time experiment. The manufacturer's instruction for the heat cycler was followed to conduct reactions in a 20 µL volume. DNA targets were amplified and analysed using a Quant Studio ™ 5 Real-Time PCR system. Table 1 contains the primer sequences used to amplify target genes.

Gene	Forward primer sequence (5′–3′)	Reverse primer sequence (5′–3′)
α-MHC	TGAGCATTCTCCTGCTGTTTC	ACACACGCGCACACACTAGCA
β-MHC	ATCCCTCAAGGTCACACAAGG	CTCCAGGTCTCAGGGCTTCAC
α-actinin	ACCGAGCATGGCTACAGCGTCACC	GTGGCCATCTCTTGCTCGGAGTCT
Bip	CGAGGCGTATTTGGGAAAGA	CAGCAATAGTGCCAGCATCC
ATF-6	TCAGCTGATGGCTGTCCAGT	AACTTCCAGGCGAAGCGTAA
Cas-9	ACGTGAACTTCTGCCCTTCC	GGTCGTTCTTCACCTCCACC
Cas-3	GTGGAACTGACGATGATATGGC	CGCAAAGTGACTGGATGAACC
Bcl-2	GGACAACATCGCTCTGTGGA	CATCCCAGCCTCCGTTATCC
CHOP	GCACCTCCCAAAGCCCTCGC	CCGTTTCCTAGTTCTTCCTT
PDI	TACGATGGCAAATTGAGCA	CTTCCACCTCATTGGCTGTT
B-actin	GCCAACCGTGAAAAGATGACCC	AGTGGTACGACCAGAGGCATAC

Table 1. Rat primer sequences for RT-PCR.

ΔΔCt was computed for each sample, and mRNA expression levels were shown by 2-ΔΔCt. The amount of PCR product was assessed as fluorescence signal intensity after standardising to β-actin as an internal reference.

Western blot

The expression of the target proteins was analyzed using western blotting. In summary, total protein was obtained by lysing cells/tissue following treatment with RIPA. After centrifugation, the supernatant was collected, and the protein content was determined using the Pierce BCA Protein Assay Kit. Equivalent protein-containing samples were electrophoresed for 90 min on 10% SDS-PAGE gels, and the separated proteins were wet-transferred to nitrocellulose (NC) membranes. Immunoblots were performed with appropriate antibodies: Calsequestrin (1:1000 CST), Troponin I (1:1000), Bip (1:1000 CST), CHOP (1:1000 CST), PDI (1:1000 CST), AKT (1:1000 CST), pAKT (1:1000 CST), pGSK 3β (1:1000 CST), GSK 3β (1:1000 CST), ERK1/2 (1:1000 CST), p-ERK1/2 (1:1000 CST), Caspase 9 (1:1000 CST), and β-actin (1:1000 CST). The membranes were incubated with the primary antibodies overnight at 4 °C after blocking with 5% skim milk in tris-buffered saline (TBST) for 1 h at 37 °C. The following day, the membranes were incubated with horseradish peroxidase-conjugated anti-mouse and anti-rabbit IgG secondary antibodies (1:2500, CST) for 1 h at room temperature after being rinsed with TBST three times. Protein bands were visualized using enhanced chemiluminescence (Biorad ChemiDoc™ MP Imaging System). The optical density (OD) of the reaction zones was calculated using ImageJ image analysis software (NIH, Bethesda, MD, USA).

Statistical analysis

GraphPad Prism, version 9 for PC (GraphPad Software, San Diego, CA, USA), was utilized for statistical analyses. Data are presented as mean ± SD. Unless otherwise specified, all experiments were performed at least four times. Statistical analyses included one-way ANOVA, t-test, and Tukey's test.

Results

Confirmation of differentiated cardiomyocytes

Significant morphological alterations under a microscope revealed that H9c2 cells had differentiated into cardiomyocytes. Differentiated H9c2 cells displayed elongated, spindle-like and orderly striated structures, indicative of adult cardiomyocytes, when compared to undifferentiated cells, which maintained a rounded and irregular form (Fig. 1. **A.**). ISO stimulation of differentiated H9c2 cardiomyocytes resulted in a significant decrease in cell viability, as determined by MTT assay (Fig. 1. **B.**). Morphological analysing indicated significant cellular alterations, such as cell shrinkage, abnormal forms, and membrane blebbing. Quantitative RT-PCR revealed that cardiomyocyte-specific genes were upregulated in differentiated H9c2 cells. Notably, the expression levels of genes such as alpha myosin heavy chain (α-MHC) (Fig. 1. **F.**), beta myosin heavy chain (β-MHC) (Fig. 1. **G.**) and β-actinin (Fig. 1. **H.**) were significantly increased, confirming the successful differentiation of the cells. Western blotting results further supported the differentiation process (Fig. 1. **C.**). The protein levels of key cardiac markers, including Calsequestrin (Fig. 1. **D.**) and Troponin I (Fig. 1. **E.**) were markedly elevated in differentiated H9c2 cells compared to undifferentiated controls.

Rob reduced ISO-induced cytotoxicity in H9c2 cells

The cardiotoxicity of different Rob concentrations on H9c2 cardiomyoblasts was determined using the MTT assay. The cells were treated with different concentrations of Rob (0–50 μg/ml) for 24 h (Fig. 2. **A**). The results clearly revealed that treatment with Rob alone had no effect on cell viability, indicating that Rob was not cytotoxic to the relevant cell line at any tested dose. After 24 h at a dosage of 50 μg/ml, cell viability remained at 95%. To test Rob's protective effects against ISO-induced oxidative stress, we used concentrations of 50 μg/ml or less for 24 h of treatment.

To study the protective effects of Rob on cardiomyocytes, cells were pre-treated with Rob (1, 5, 10, 25, and 50 μg/ml) for 24 h before being exposed to 100 μM ISO (Decreases cell viability to 50%) (Fig. 2. **B.**). Rob (1, 5, 10, 25, and 50 μg/ml) improved H9c2 cell viability to 63.45%, 69.82%, 76.35%, 85.45%, and 90.19%, respectively. These data suggest that Rob may be capable of protecting H9c2 cells from oxidative stress-induced cell damage.

Rob ameliorates ISO-induced geometric and morphological changes in H9c2 cells

The level of morphological alterations in H9c2 cells was assessed, and cytomorphology was done using a phase-contrast microscope (Fig. 2.**C.**). H9c2 cells treated with 100 μM ISO demonstrated considerable morphological alterations. Cells in the control and Rob-treated groups had intact plasma membranes, elongated fusiform and spindle shapes, and spherical nuclei. ISO-pronounced cell injury, characterised by loss of adhesion and the appearance of rounded cells. ISO treatment caused cellular shrinkage, membrane blebbing, and structural alternations, which were characterised as a rise in cell size and shape owing to changes in protein synthesis and metabolism. Pre-treatment with Rob dramatically improved these ISO-induced morphological changes, restoring cell integrity, retaining cell shape, minimising intercellular gaps, and preserving nuclear morphology.

Effect of Rob on antioxidant enzymes

When cells were treated with 50 μg/ml Rob against ISO, SOD and CAT levels increased. These results demonstrate that Rob's natural anti-oxidant activity protects cells from ISO-induced toxicity (Fig. 2. **F**, **G.**).

Rob reduced the production of intracellular ROS

H9c2 cells treated with 100 μM ISO for 24 h produced considerably more ROS than untreated cells. However, pre-treatment with Rob significantly reduced ROS levels. (Fig. 3. **A.**). FACS analysis (Fig. 3. **B-F.**) was also employed to monitor ROS levels. The fluorescence shift from left to right indicates that intracellular ROS levels increased

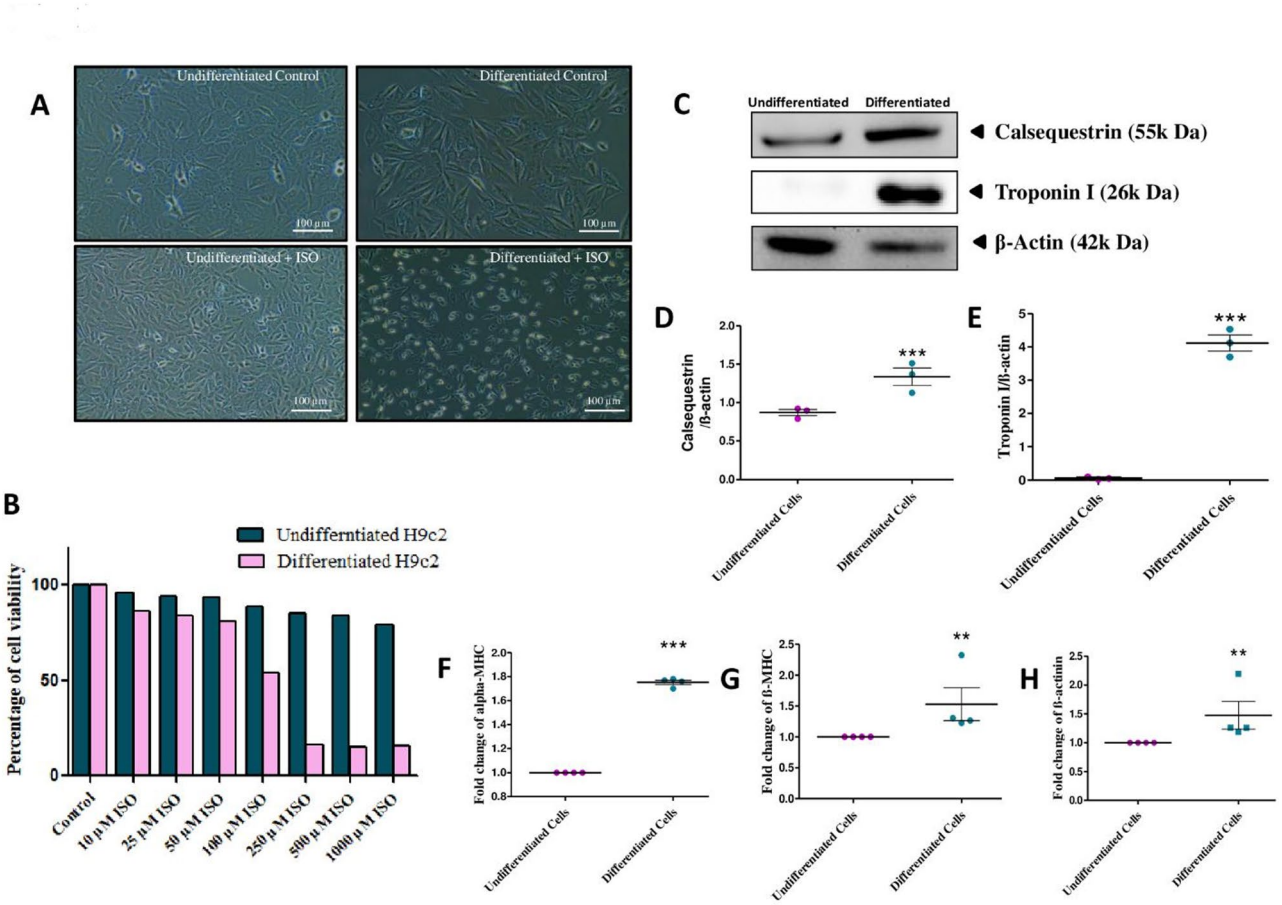

Fig. 1. Confirmation of differentiation of H9c2 (**A**) Morphological changes upon 100 µM ISO treatment under inverted microscopy after treatment (×100 µm magnification). The elongated, spindle-shaped morphology indicative of cardiomyocyte differentiation is visibly altered upon ISO exposure. (**B**) Cytotoxic effect of ISO at micromolar concentration on H9c2 cardiomyocytes was evaluated by MTT assay. A concentration-dependent decrease in cell viability, indicating ISO's detrimental effect on H9c2 cells. (**C**) Western blot chemiluminescence. (**D**) Graphical representation of Calsequestrin, (**E**) Graphical representation of Troponin I. mRNA expression of (**F**) α-MHC, (**G**) β-MHC and (**H**) β-actinin. Results indicated the successful differentiation of H9c2. *Denotes statistically significant differences in comparison with control: ns > 0.05, $^{*}p < 0.05$, $^{**}p < 0.01$, $^{***}p < 0.001$. Data are presented as mean ± SD of three and four independent. experiments. SD, standard deviation.

during 24 h of ISO therapy (Fig. 5. **C.**). Statistical analysis demonstrated that the proportion of cells with elevated ROS in the ISO-treated group was 78 ± 2.5%, but declined to 65 ± 3.1% with Rob pre-treatment (Fig. 3. **G.**). These findings suggest that pre-treatment with Rob significantly reduces intracellular ROS generation. The full original image of DCFH-DA staining is presented in supplementary data (**Fig. S2.)**

Rob reduced the number of early and late apoptotic cell

In the control and Rob-treated groups, cells showed no significant evidence of apoptosis and maintained a normal morphology with green fluorescence. The experimental group treated with ISO showed a significant increase in apoptotic cells. Rob pre-treatment dramatically decreased the amount of ISO-induced apoptotic cells at both the early and late stages. The number of necrotic cells also decreased, and the cells had a more consistent shape than the ISO group. Rob pre-treatment boosted the number of viable cells, as evidenced by the reduction of AO/EB staining associated with apoptosis and necrosis (Fig. 4. **A.**). The full original image of AO/EB staining is presented in supplementary data (**Fig. S3.)**

H9c2 cells were also stained with Annexin V-FITC and propidium iodide (PI) and analyzed using FACS to assess apoptosis and necrosis. In the ISO-treated group, there was a substantial increase in apoptotic and necrotic cells. FACS analysis revealed a significant population of early apoptotic cells (Annexin V+/PI-) and late apoptotic cells (Annexin V+/PI+). This indicates that ISO induces both early and late stages of apoptosis as well as necrosis in H9c2 cells. Rob pre-treatment markedly reduced the population of early apoptotic (Annexin V+/PI-) and late apoptotic (Annexin V+/PI+) cells (Fig. 4B-D.). The full original image of FACS analysis is presented in supplementary data (**Fig. S4.)**

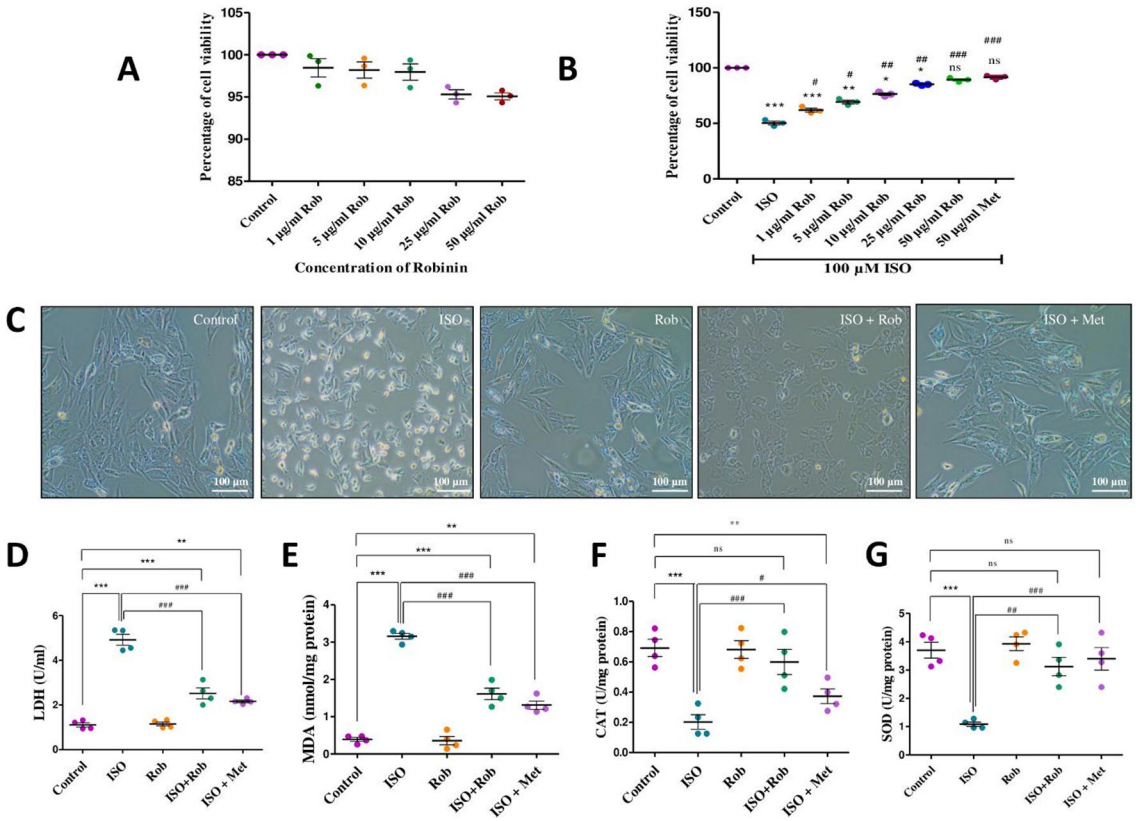

Fig. 2. Cytotoxic effects of Rob on H9c2 cell line, and protective effect of Rob to ameliorate ISO induced stress in H9c2 cardiomyocyte. (**A**) Cytotoxic effect of Rob at microgram concentration on H9c2 cardiomyocytes was evaluated by MTT assay, confirming its safety profile at tested doses. (**B**) Protective effect of Rob on 100 µM ISO induced oxidative stress on H9c2 cardiomyocytes evaluated by MTT assay, showing a dose-dependent restoration of cell viability. (**C**) Morphological observations of cardiomyocytes under inverted microscopy after treatment, illustrate ISO-induced cellular damage and Rob-mediated morphological preservation (×100 µm magnification). Effect of Rob on oxidant and antioxidant enzyme levels, measured by enzyme assay kit, (**D**) LDH, (**E**) MDA, (**F**) CAT and (**G**) SOD. Rob pre-treatment significantly reduced ISO-elevated levels of LDH and MDA, while restoring the activities of antioxidant enzymes CAT and SOD, indicating its potent cytoprotective and antioxidant role. *Denotes statistically significant differences in comparison with control: ns > 0.05, $*p < 0.05$, $**p < 0.01$, $***p < 0.001$. #Denotes statistically significant differences in comparison with ISO group: $\#p < 0.05$, $\#\#p < 0.01$, $\#\#\#p < 0.001$. Data are presented as mean ± SD of four independent experiments. SD, standard deviation.

Effect of Rob on body weight, heart weight, and heart-to-Body weight ratio

There were no statistically significant variations in body weight between groups. Figure 5A. shows the treatment procedure for the animal experiment. The heart size of rats treated with ISO increased, whereas Rob pre-treatment helped maintain a normal heart size (Fig. 5B.**)**. Additionally, the ISO-administered groups did not show any significant increase or decrease in body weight compared to the control group (Fig. 5C.). When rats were pre-treated with Rob, their heart weight and heart weight to body weight ratios dropped dramatically compared to those receiving ISO treatment (Fig. 5D.). Compared to the normal control groups, the ISO-administered groups had substantially greater heart weight and heart weight to body weight ratios (Fig. 5E.).

Effect of Rob on marker enzymes

The levels of diagnostic markers MDA in the cell and cardiac tissue homogenates, LDH in the culture supernatant, CK-MB, LDH, and SGOT in serum were increased significantly (Fig. 2. **D.**, Fig. 2E.) and (Fig. 5. **F-I.**). In compared with the ISO, Rob pre-treatment resulted in a significant reduction in the levels of all diagnostic marker enzymes.

Effect of Rob on myocardial tissue damage

(Fig. 6. **A.**) illustrates typical images of infarction size stained with TTC. While ISO therapy resulted in a larger region of infarction (unstained section), the cardiac section of Rob-treated group revealed a considerable quantity of tissues that stained positively, suggesting tissue viability.

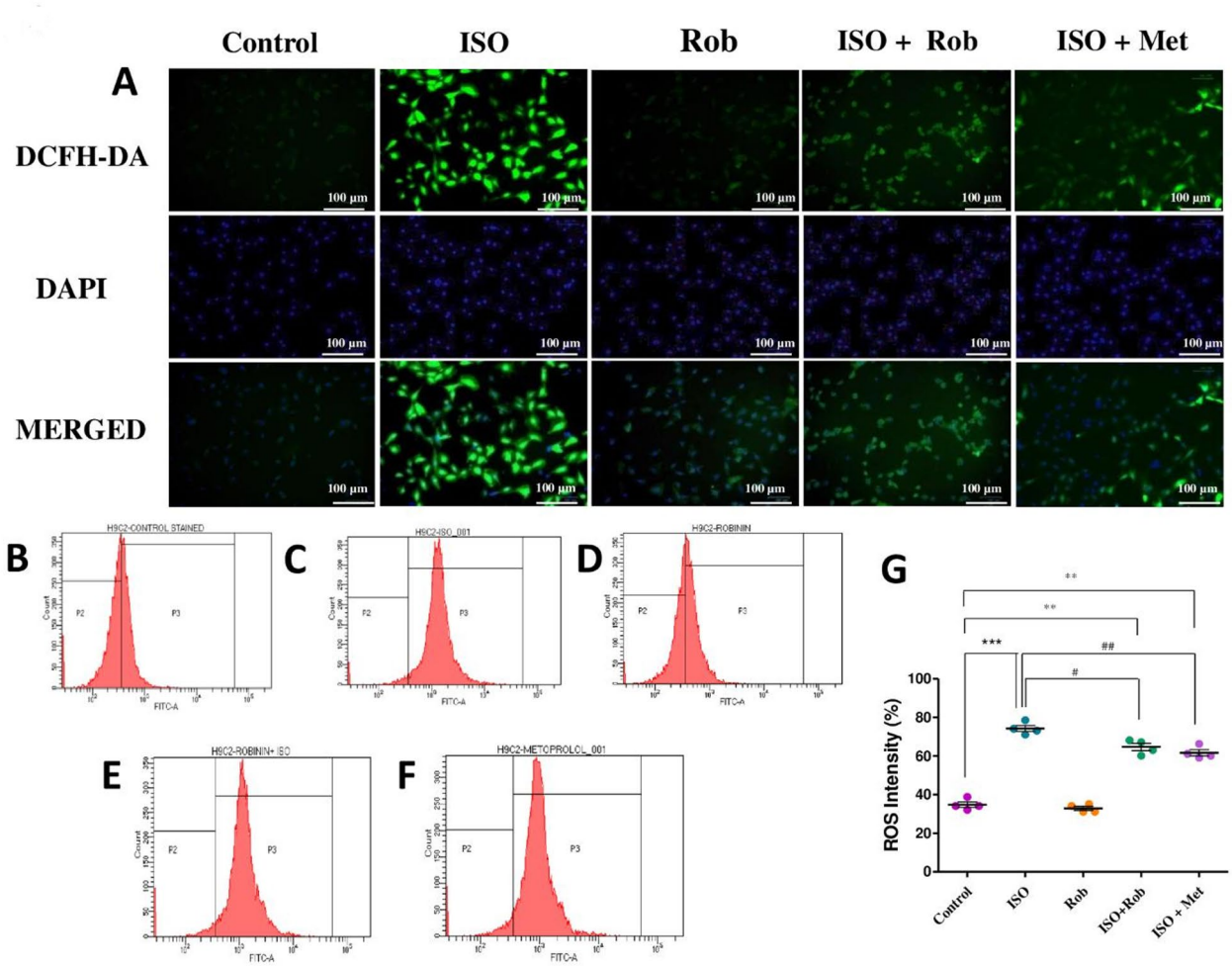

Fig. 3. Effect of Rob on reducing intracellular ROS production. (**A**) H9c2 cells were pre-incubated with $DCFH_2$-DA (10 µM) for 15 min to detect ROS generation. After the pre-incubation, cells were treated with or without Rob and Met for an additional 24 h, followed by ISO treatment. The generation of ROS was visualized using a fluorescence microscope, where green fluorescence indicates the presence of ROS (Bar = 100 µm). Nuclei were counterstained with DAPI (blue), and the images were merged to illustrate the overlap between ROS generation and cellular morphology. The fluorescence intensity of $DCFH_2$-DA corresponds to the levels of intracellular ROS, providing a visual representation of the oxidative stress induced by ISO and the protective effects of Rob and Met. Intracellular ROS generation in H9c2 cells measured by FACS. (**B**) Control, (**C**) ISO, (**D**) Rob (**E**) Rob + ISO and (**F**) Met + ISO. (**G**) Graphical representation of percentage of ROS production. The data show the mean fluorescence intensity of DCF. The analysis reveals how pre-treatment with Rob and Met affects ROS production in response to oxidative stress induced by ISO. *Denotes statistically significant differences in comparison with control: ns > 0.05, $*p < 0.05$, $**p < 0.01$, $***p < 0.001$. #Denotes statistically significant differences in comparison with ISO group: $\#p < 0.05$, $\#\#p < 0.01$, $\#\#\#p < 0.001$. Data are presented as mean ± SD of four independent experiments. SD, standard deviation.

Effect of Rob on histological changes

The histopathological examination of the untreated and Rob alone treated group's left ventricular heart section revealed a usual myofibrillar structure with striations, branching, and consistency with the surrounding myofibrils (Fig. 6B., Fig. 6D.). ISO-injected rats showed significant myofibrillar degeneration, interstitial swelling, and neutrophil granulocyte invasion (Fig. 6C.). In comparison to the ISO-induced group, the morphology of the cardiac muscle fibres was rather intact, with no evidence of localised necrosis in the tissue sections from the Rob pre-treated group (Fig. 6E.). However, there was minimal neutrophil granulocyte infiltration, interstitial oedema, and some discontinuity with adjacent myofibrils.

Gene expression analysis

Quantitative RT-PCR was performed to evaluate the expression levels of key genes involved in apoptosis and ER stress (Table 1**).** ISO treatment markedly increased the expression of ER stress markers, including CHOP (Fig. 7A., Fig. 8A.), Bip (Fig. 7B., Fig. 8B.), ATF 6 (Fig. 7C., Fig. 8C.) and PDI (Fig. 7D., Fig. 8D.). Rob pre-treatment significantly reduced the expression of these markers, suggesting a protective effect against ISO-

induced ER stress. There was a significant upregulation of pro-apoptotic genes such as Caspase 3 (Fig. 7E., Fig. 8E.) Caspase 9 (Fig. 7F., Fig. 8F.) and Bax (Fig. 7G., Fig. 8G.) in the ISO-treated group compared to the control group. Conversely, the expression of the anti-apoptotic gene Bcl-2 (Fig. 7H., Fig. 8H.) was significantly downregulated in the ISO group. Pre-treatment with Rob normalized the expression levels of these genes, indicating a reduction in apoptosis.

Protein expression analysis

Western blotting was conducted to assess the protein levels corresponding to the apoptotic, ER stress, and survival pathways (Fig. 7I., Fig. 7M., Fig. 7O., Fig. 8I., Fig. 8M., Fig. 8O). ISO-treated cells showed elevated levels of Bip (Fig. 7J., Fig. 8J), CHOP (Fig. 7K., Fig. 8K), and PDI (Fig. 7L., Fig. 8L) proteins, indicative of ER stress. Rob pre-treatment significantly lowered the levels of these ER stress markers. Protein levels of Caspase 9 (Fig. 7N., Fig. 8N) were significantly increased in the ISO-treated group. Rob pre-treatment significantly decreased Caspase 9 levels, demonstrating its anti-apoptotic effect. ISO treatment resulted in reduced levels of phosphorylated AKT (Fig. 7P., Fig. 8P), Glycogen synthase kinase-3β (GSK 3-β) (Fig. 7Q., Fig. 8Q), and increased level of ERK1/2 phosphorylation (Fig. 7R., Fig. 8R) correlating with decreased cell survival. Rob pre-treatment increased the phosphorylated AKT and GSK 3-β levels, suggesting a restoration of survival and anti-apoptotic capacity. The uncropped, untouched and full original image of western blot is presented in supplementary data (**Fig. S1.).**

Discussion

This study elucidates the novel protective role of Rob against ISO induced MI in H9c2 cardiomyocytes, providing insights into its potential therapeutic applications. The processes of ISO-induced myocardial ischaemic damage are complicated, involving cardiomyocyte apoptosis and autophagy, ERS, intracellular calcium excess and oxidative stress, among others.

Significant morphological alterations, as well as activation of cardiomyocyte-specific genes and proteins, indicated H9c2 cell differentiation into cardiomyocytes. These differentiated cells provided a good model for investigating cardiac injury and Rob's preventive effects. Differentiated cardiomyocytes closely resemble adult heart cells in terms of physiological characteristics and functional responses, making them more valuable for simulating cardiac diseases and evaluating treatment methods. They feature discrete cardiac markers and structural characters , enabling for accurate analysis of gene and protein expression variations in experimental conditions. Non-differentiated cells lack these characteristics, making them less valuable for studying heart disorders and drug response[13].

When ISO is supplied in supramaximal dosages, the heart exhibits morphological and functional changes that are similar to the pathological irregularities associated with local MI that occur in humans. These alterations include subendocardial myocardial ischemia, hypoxia, and necrosis which leads to fibroblastic hyperplasia with lower myocardial compliance and suppression of diastolic and systolic function[14]. One of the key contributing causes of ISO-induced cardiac damage has been recognised as the formation of extremely cytotoxic free radicals through the auto-oxidation of catecholamines[15]. According to studies, the auto-oxidation of excess catecholamines leads to the peroxidation of membrane phospholipids mediated by free radicals, which causes changes in the permeability of the heart membrane, intracellular calcium overload, and irreversible damage[16]. By activating beta-1 receptors on myocardial cells, ISO also enhances the force of contraction of the heart muscle (positive inotropic effect). This increased contractility has the potential to increase myocardial oxygen consumption, which exacerbates the supply and demand imbalance for oxygen, a major cause of myocardial ischemia and injury[17].

The current study on cell viability discovered that ISO treatment significantly reduced cell viability, as seen by a loss of adhering nature and the formation of rounded cells, suggesting progressive cell death. When compared to ISO-treated cells, cells pre-treated with Rob showed a significant increase in cell viability while maintaining normal morphology. It has also been demonstrated that when H9c2 cells are exposed to higher levels of ISO, they experience mitochondrial swelling, extensive cytoplasm vacuolization, and nuclear swelling with membrane rupture. Our results show that Rob efficiently decreases ISO-induced cytotoxicity and morphological changes. This suggests that Rob helps preserve cellular integrity under oxidative stress conditions.

ISO significantly enhanced the production of ROS in H9c2 cells, as seen by increased fluorescent intensity. While the cells treated with Rob produced lower ROS levels than ISO-alone cells. Rob significantly reduced ROS formation in H9c2 cells, which might be attributable to its antioxidant properties. The cell line treated with ISO and Rob was also stained with AO/EB to qualitatively determine apoptotic activity. Cells showing green to orange fluorescence were considered apoptotic, depending on nuclear morphology and membrane integrity. The necrotic cells seemed degraded and deformed, with stains dispersed asymmetrically across them. The outcomes of this study clearly indicated that cells treated with ISO undergo cell death, as seen by a higher percentage of red-colored cells compared to untreated cells. Cells treated with Rob showed a significant reduction in cell death, as evidenced by a decreased number of red-colored cells.

In the rats treated with ISO, we found that there was a notable rise in both the heart weight and the heart weight to body weight ratio. According to Patel et al. the observed rise in heart weight in ISO-induced rats may be caused by increased water content, oedematous intramuscular space, and widespread cardiac muscle fibre necrosis, which is followed by inflammatory cells invading injured tissues[18]. In rats induced with ISO, the Rob treatment resulted in a considerable reduction in heart weight.

TTC dye, which creates a red formazan precipitate when dehydrogenase enzyme systems are intact but does not stain the infarcted myocardium because it lacks dehydrogenase activity, can be used to detect the degree of the MI. Loss of membrane integrity and dehydrogenase leakage might be connected to the infarction region[19]. Rats that were exposed to ISO had larger myocardial infarcts with reduced TTC absorption ability, which suggested a substantial myocardial dehydrogenase leak. The Rob pre-treatment prevented the loss of

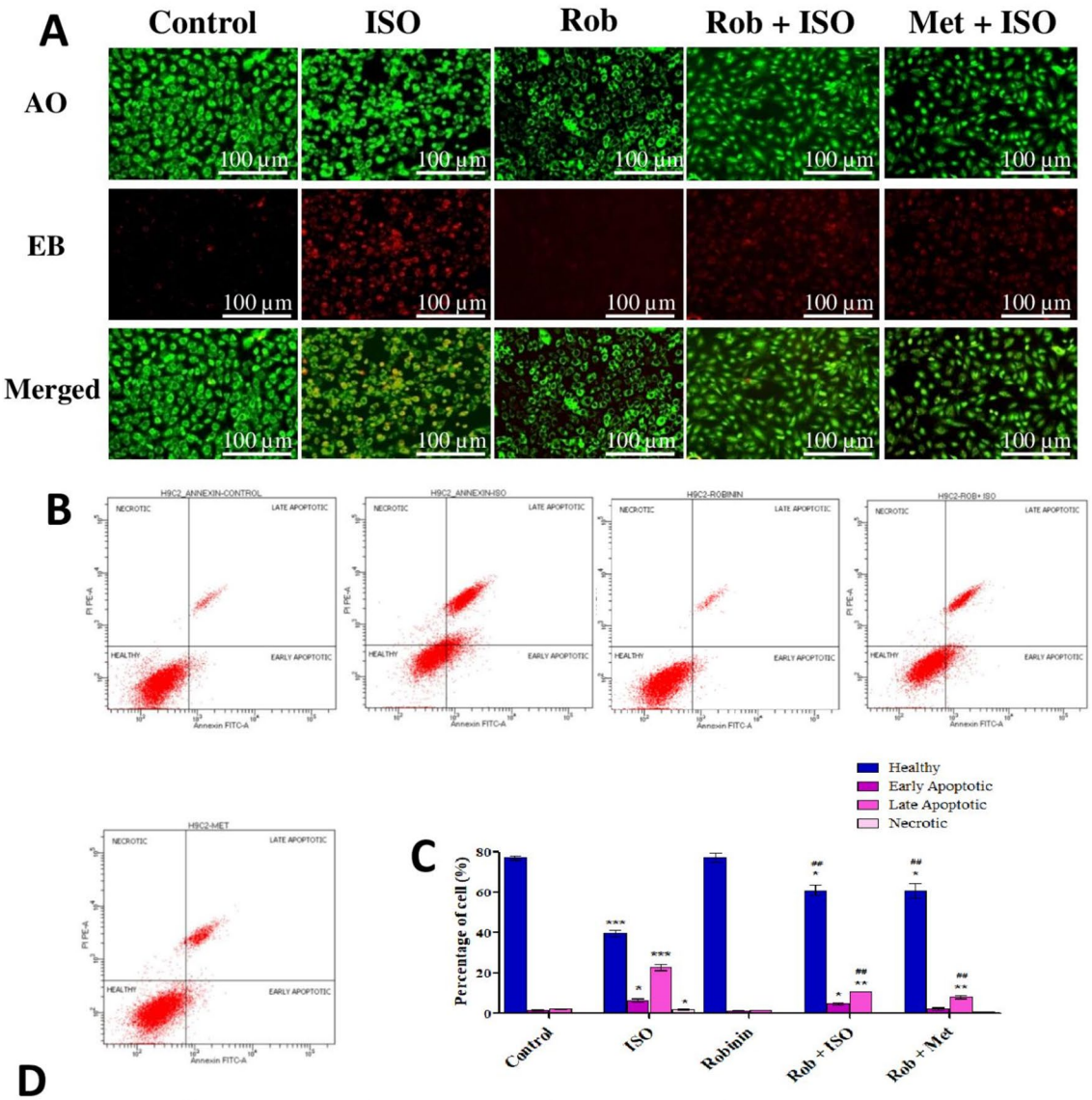

D

Population	Control	ISO	Robinin	Rob + ISO	Met + ISO
Healthy	78.00 %	38.2 %	79.6%	63.7 %	64.6 %
Early Apoptotic	1.7 %	5.8 %	1.5 %	4.2 %	3.00 %
Late Apoptotic	2.6 %	24.3 %	1.7 %	10.9 %	7.1 %
Necrotic	0.00 %	2.5%	0.0 %	0.6 %	0.5 %

dehydrogenases caused by ISO, the group showed a much lower level of infarct size, further demonstrating the combination's superior protection against heart injury.

The levels of CK-MB, LDH, SGOT and MDA are sensitive indicators that can be used to determine the extent of MI. This was presumably related to changes in membrane permeability and disintegrity caused by ISO-induced MI. Increased activity of these markers in the serum/tissue is suggestive of cellular injury, loss of membrane permeability, and/or loss of functional integrity[20,21]. The present investigation has revealed a noteworthy rise in the levels of CK-MB, LDH, SGOT and MDA in rats that were induced with ISO which has been decreased by Rob treatment. For oxidative stress in intracellular organelles to be effectively removed, the balance between enzymatic antioxidants and free radicals is crucial[22]. However; the generation of ROS can dramatically disrupt this balance in pathological conditions such as MI by putting the extra workload on the antioxidant defence system. The drop in SOD and CAT activity might be attributed to the increased utilisation

Fig. 4. Assessment of apoptosis and necrosis in H9c2 cells using AO/EB staining. Following treatment, cells were stained with acridine orange (AO) and ethidium bromide (EB) to differentiate between viable, early apoptotic, late apoptotic, and necrotic cells. AO stains viable cells green, while EB stains dead or dying cells red. (**A**) Representative fluorescence images showing the different cell populations. Viable cells appear green, early apoptotic cells exhibit yellow-green fluorescence, and late apoptotic or necrotic cells show red fluorescence. The images were captured using a fluorescence microscope (Bar = 100 µm). (**B**) Analysis of apoptosis and necrosis in H9c2 cells using Annexin V-FITC and propidium iodide (PI) staining (**C**) Graphical representation of the percentage of each cell type (**D**) Table showing the number of early, late apoptotic and necrotic cell populations in response to oxidative stress. *Denotes statistically significant differences in comparison with control: ns > 0.05, *$p < 0.05$, **$p < 0.01$, ***$p < 0.001$. #Denotes statistically significant differences in comparison with ISO group: #$p < 0.05$, ##$p < 0.01$, ###$p < 0.001$. Data are presented as mean ± SD of four independent experiments. SD, standard deviation.

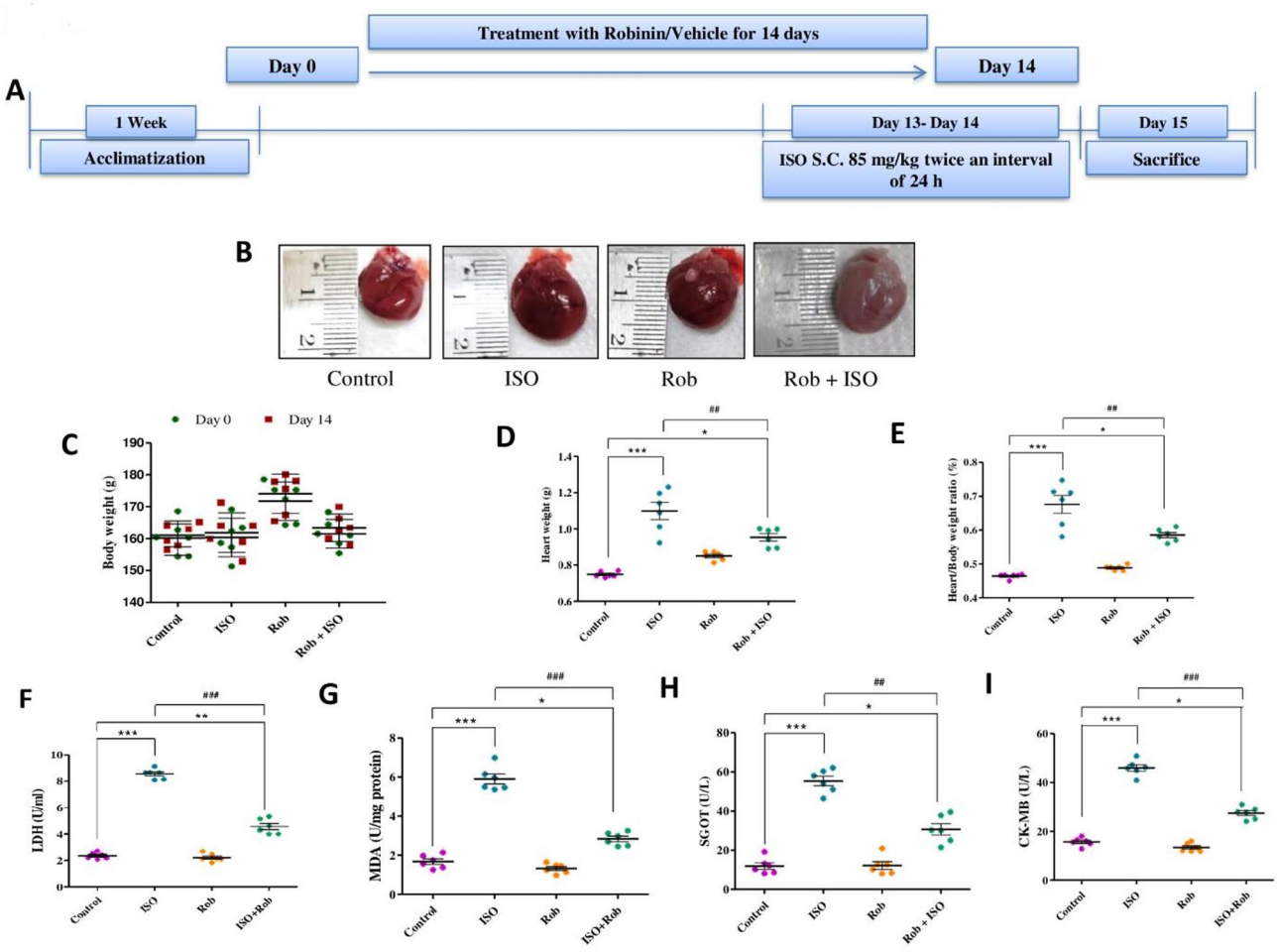

Fig. 5. Schematic representation of the experimental design for MI rat model induced by ISO (**A**) Timeline of the study design. (**B**) size of heart. (**C**) Effect of Rob on the body weight. (**D**) Effect of Rob on the heart weight. (**E**) Effect of Rob on the heart to body weight. Effect of Rob on serum/tissue marker levels, measured by enzyme assay kit, (**F**) LDH, (**G**) MDA, (**H**) SGOT and (**I**) CK-MB. Rob treatment significantly reduced elevated levels of myocardial injury markers in ISO-induced rats. *Denotes statistically significant differences in comparison with control: ns > 0.05, *$p < 0.05$, **$p < 0.01$, ***$p < 0.001$. #Denotes statistically significant differences in comparison with ISO group: #$p < 0.05$, ##$p < 0.01$, ###$p < 0.001$. Data are presented as mean ± SD of six independent experiments. SD, standard deviation.

of these enzymes for ROS scavenging, as well as inactivation by high ISO oxidants. In comparison to ISO groups, pre-treatment with Rob significantly boosts the activities of SOD and CAT.

When compared to the ISO-induced heart, a histopathological analysis of the tissue of control group revealed obvious integrity of the heart's cell membrane along with no signs of localised necrosis or inflammatory cell infiltration. Rats treated with ISO had heart muscle fibre separation and a significant neutrophil granulocyte

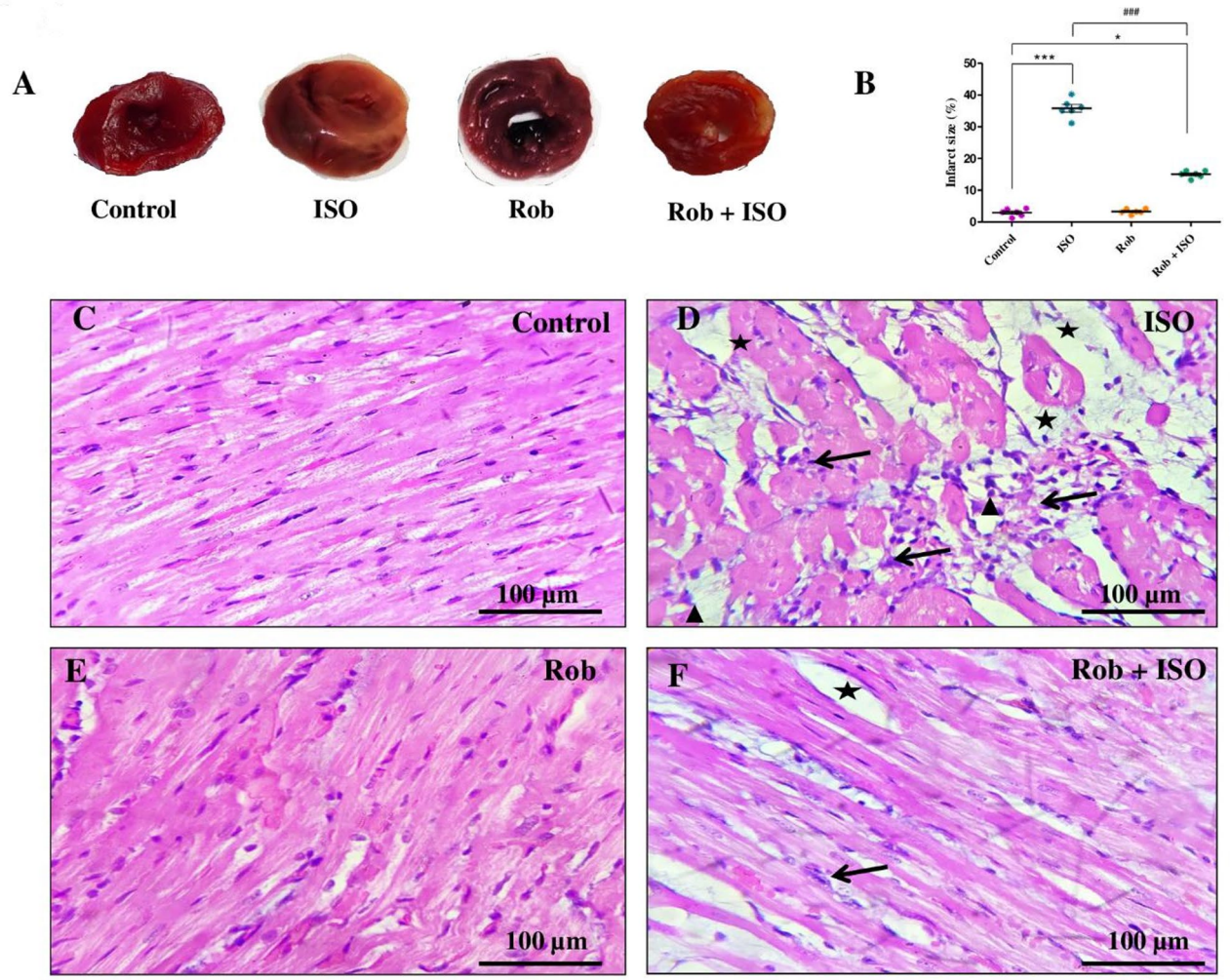

Fig. 6. **(A)** Triphenyl Tetrazolium Chloride stained transverse slices of the heart of Control, ISO treated, Rob and Rob + ISO treated groups. TTC stains viable cardiac muscle deeply red, whereas regions of infarction are pale. Photomicrograph of H&E stained sections of left ventricular tissues, (B) Quantitative analysis of infarct size. Infarct size was calculated by the ratio of the infarction area to the total left ventricular section area and quantified using ImageJ software. (C) Cardiomyocytes shows regular striated structure in control group. (D) In ISO group cardiomyocytes shows altered morphology, the nuclei are irregular in shape, the cytoplasm is devoid of organelles (star), damaged myocytes presented with loss of cellular organization, diffused/focal inflammatory infiltrate ( ). (E) Rob alone group shows morphology similar to that of control. (F) In Rob + ISO group heart tissue with improved structural and morphological features similar to healthy control. Scale bar: 100 µm. Data are presented as mean ± SD of six independent experiments. SD, standard deviation.

infiltration. Further evidence of the cardioprotective benefits of Rob was provided by the Rob + ISO group's decreased inflammatory cell infiltration and normal cardiac muscle fibre architecture.

Apoptosis has been connected to both inflammation and oxidative stress. Pro-apoptotic proteins like Bax and anti-apoptotic proteins like Bcl-2 govern the intrinsic route of apoptosis, which is triggered by ROS. As a result, apoptosis and caspase-8 activation occurs first, followed by caspase-3 activation[23]. Therefore, elevated oxidative stress and inflammation may be the cause of the apoptotic alterations seen in the ISO group. Consistent with other research, ISO led to a considerable rise in cardiac Bax levels and a significant decrease in Bcl-2 levels. It is commonly known that the acute stage of MI involves both necrosis and apoptosis[24]. The Bcl-2 family's pro- and anti-apoptotic proteins interact to integrate various death and survival signals, ultimately determining the destiny of the cells[25]. Apoptotic signalling in mitochondria is triggered by an excess of ROS in infarction regions during acute MI. This activation of Bax, a pro-apoptotic Bcl-2 family protein, is a result of this activation. The majority of Bax is found in the cytosol in healthy cells, but when apoptotic signalling begins, activated Bax quickly moves to the mitochondria, where it undergoes a conformational change and joins forces with Bak to create protein-permeable pores on mitochondrial membranes[26].

Although catecholamines regulate cardiac function, high levels cause ischemic heart disease such as MI, cardiac hypertrophy, and heart failure. This is a consequence of aberrant β-adrenergic activity[27]. This indicates that excess production of ROS induced by ISO triggered ER stress. Furthermore, Rob treatment ameliorated

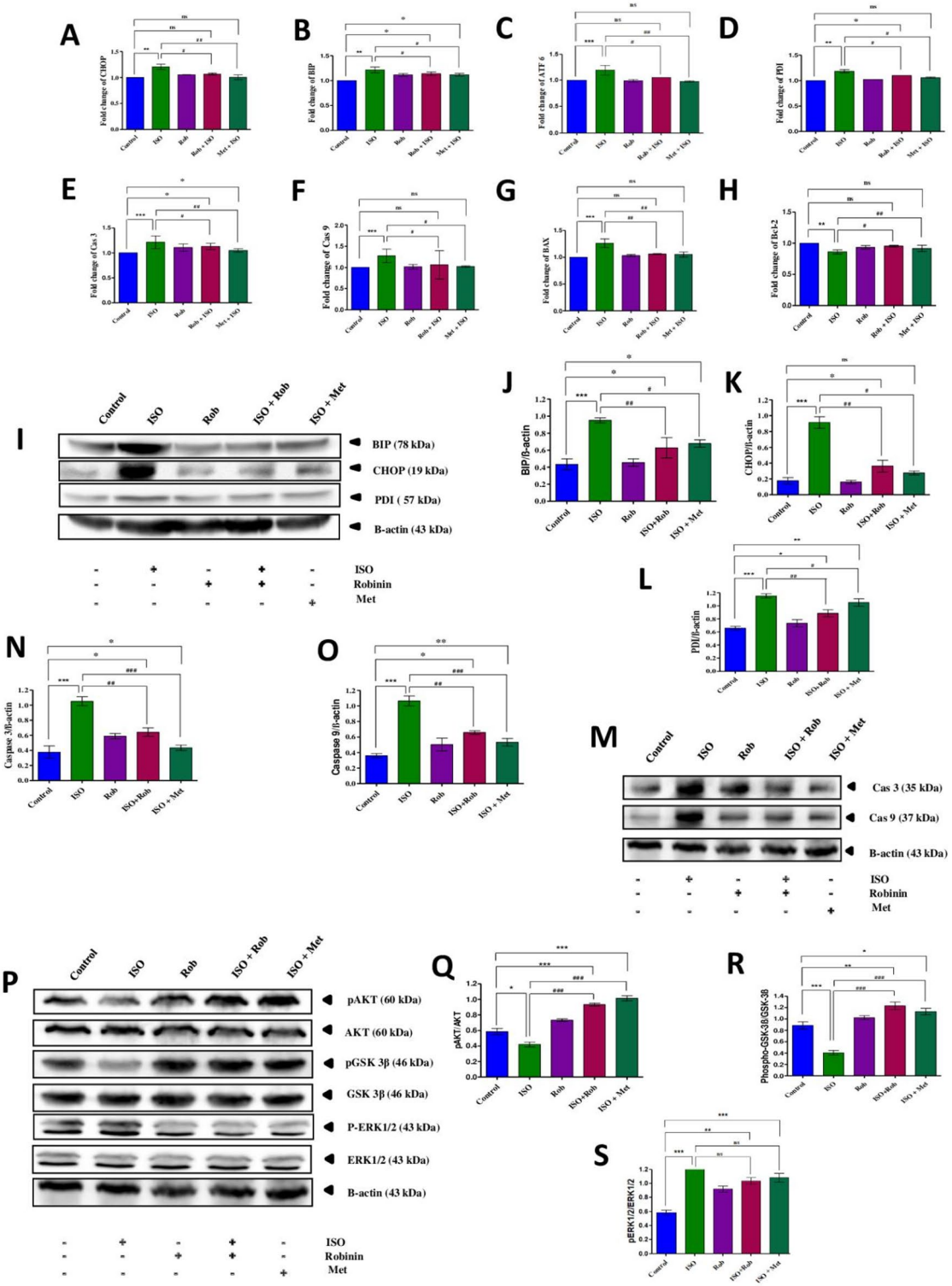
A
B
C
D
E
F
G
H
I
Control
ISO
Rob
ISO + Rob
ISO + Met
BIP (78 kDa)
CHOP (19 kDa)
PDI (57 kDa)
B-actin (43 kDa)
ISO
Robinin
Met
J
K
L
M
Cas 3 (35 kDa)
Cas 9 (37 kDa)
B-actin (43 kDa)
N
O
P
pAKT (60 kDa)
AKT (60 kDa)
pGSK 3β (46 kDa)
GSK 3β (46 kDa)
P-ERK1/2 (43 kDa)
ERK1/2 (43 kDa)
B-actin (43 kDa)
Q
R
S

◀**Fig. 7**. Effects of Rob on ER-stress related gene expression, apoptotic, and anti-apoptotic genes in H9c2 through real-time PCR. Genes were normalized with β-actin and results are expressed as fold change from control, and ISO. mRNA expression of **(A)** CHOP, **(B)** Bip, **(C)** ATF 6, **(D)** PDI, **(E)** Cas 3, **(F)** Cas 9, (**G**) BAX and (**H**) Bcl-2 on Control, ISO and Rob pre-treated groups. Effects of Rob on ER-stress, apoptotic and survival related protein expression through western blot. **(I)** Western blot chemiluminescence of ERS related proteins. **(J)** Bip, **(K)** CHOP, and **(L)** PDI. (**M**) Western blot chemiluminescence of apoptosis related proteins. (**N**) Caspase 9 and (**O**) Western blot chemiluminescence of survival related proteins. (**P**) AKT, (**Q**) GSK-3β and (**R**) ERK1/2. Equal protein loading was confirmed by β-actin. Densitometry was performed with the ImageJ software and densitometric analysis of the observed bands was intensity normalized to β-actin. *Denotes statistically significant differences in comparison with control: ns > 0.05, $*p < 0.05$, $**p < 0.01$, $***p < 0.001$. #Denotes statistically significant differences in comparison with ISO group: $\#p < 0.05$, $\#\#p < 0.01$, $\#\#\#p < 0.001$. *In vitro* data are presented as mean ± SD of four independent experiments. *In vivo* data are presented as mean ± SD of six independent experiments. SD, standard deviation.

ISO-induced myocardial injury, as evidenced by improvements in histopathology and biochemical markers of oxidative stress and cardiac damage. The protective effects of Rob were evidenced by the down regulation of ER stress markers, such as CHOP, Bip, ATF 6, and PDI, at mRNA and protein levels, which corresponded to decreased apoptosis and oxidative stress. Specifically, ISO treatment markedly increased ER stress and pro-apoptotic gene expression, alongside elevated ROS production and reduced antioxidant enzyme activity, which collectively induced significant cardiomyocyte damage. These findings underscore Rob's capacity to modulate ER stress and associated apoptotic pathways, positioning it as a promising candidate for the treatment of MI.

Angiogenesis is a crucial compensatory tissue response to hypoxia[28]. A number of mechanisms linked to the control of angiogenesis are activated by hypoxia, including as the Akt and HIF-1α signalling pathways. Through the regulation of several physiological processes, including angiogenesis and cell survival, Akt signalling is important in the adaptation of the body to ischemia[29]. Akt phosphorylates and inactivates pro-apoptotic factors like Bax and caspase-9, promoting cell survival. On the other hand ERK1/2 activation leads to the expression of genes involved in cell survival, repair, and regeneration, which are crucial for recovering from ISO-induced damage. However, prolonged or high-dose ISO exposure may shift ERK1/2 activation toward maladaptive remodeling or apoptosis, especially in cardiomyocytes[30].

Despite the promising findings, the study has certain limitations. The exact molecular mechanisms underlying Rob's protective effects need to be elucidated in greater detail. Although our findings indicate that Rob activates the AKT/GSK3β signaling pathway, the study does not establish a direct causal relationship. Further mechanistic investigations using pathway-specific inhibitors or gene silencing approaches are needed to confirm the role of this pathway in mediating the cardioprotective effects of Rob. In conclusion, this study highlights the novel protective role of Rob against ISO-induced myocardial damage. Rob demonstrated comparable efficacy to Met in reducing cytotoxicity, oxidative stress, apoptosis, and ERS, underscoring its promise as an alternative or complementary therapy for managing MI. Rob's ability to reduce cytotoxicity, oxidative stress, apoptosis, and ER stress, while enhancing cell survival, underscores its potential as a therapeutic agent for MI. The findings provide a strong foundation for further exploration of Rob's cardioprotective properties and its possible clinical applications. The relevance of this study lies in its potential therapeutic implications. MI remains a leading cause of morbidity and mortality worldwide, and the development of effective treatments is crucial. By demonstrating the efficacy of Rob in protecting cardiomyocytes from oxidative stress and apoptosis, this research paves the way for further investigations into its clinical applications. The findings support the potential use of Rob as a complementary therapy for patients at risk of or suffering from MI, ultimately contributing to improved cardiovascular health outcomes.

Conclusions

In conclusion, this is the first study to demonstrate that, in an ISO-induced rat model, Rob, a glycoflavanoid has cardioprotective effects. Rob mitigated myocardial oxidative stress and apoptosis, accompanied by activation of AKT and normalization of ERK signaling. Our study also suggests that Rob significantly improved all parameters linked to oxidative stress and, inflammatory status in ISO-induced MI rats. By modulating key signaling pathways involved in ER stress and apoptosis, Rob not only enhances cellular resilience against oxidative insults but also promotes overall myocardial health. These findings position Rob as a promising therapeutic agent for MI, offering a multifaceted approach to mitigating cardiac injury and enhancing recovery.

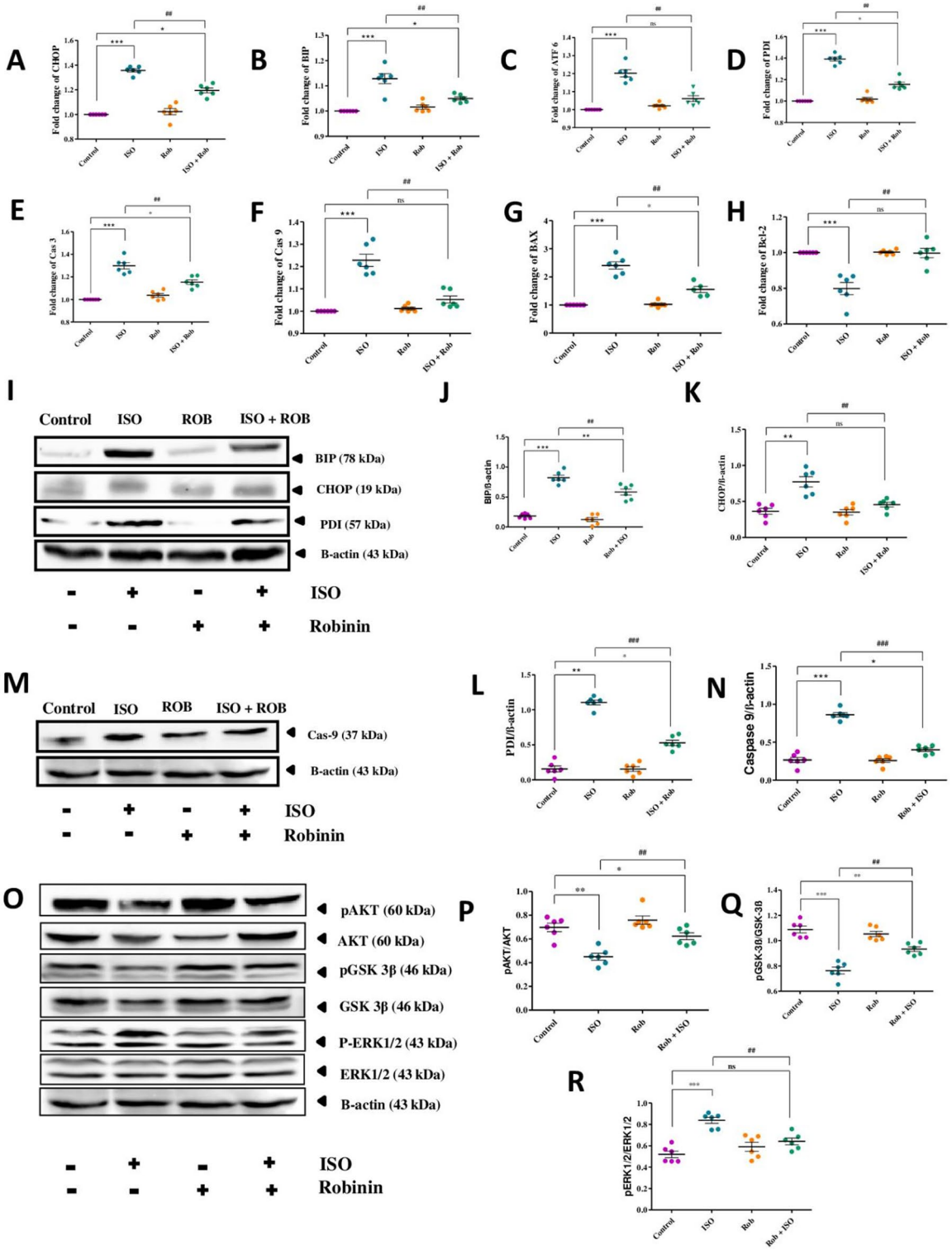
A
Fold change of CHOP
B
Fold change of BIP
C
Fold change of ATF 6
D
Fold change of PDI
E
Fold change of Cas 3
F
Fold change of Cas 9
G
Fold change of BAX
H
Fold change of Bcl-2
Control
ISO
Rob
ISO + Rob
I
Control
ISO
ROB
ISO + ROB
BIP (78 kDa)
CHOP (19 kDa)
PDI (57 kDa)
B-actin (43 kDa)
ISO
Robinin
J
BIP/β-actin
K
CHOP/β-actin
M
Cas-9 (37 kDa)
L
PDI/β-actin
N
Caspase 9/β-actin
O
pAKT (60 kDa)
AKT (60 kDa)
pGSK 3β (46 kDa)
GSK 3β (46 kDa)
P-ERK1/2 (43 kDa)
ERK1/2 (43 kDa)
P
pAKT/AKT
Q
pGSK-3β/GSK-3β
R
pERK1/2/ERK1/2

◀**Fig. 8**. Effects of Rob on ER-stress related gene expression, apoptotic, and anti-apoptotic genes in Sprague Dawley rat model through real-time PCR. Genes were normalized with β-actin and results are expressed as fold change from control, and ISO. mRNA expression of **(A)** CHOP, **(B)** Bip, **(C)** ATF 6, **(D)** PDI, **(E)** Cas 3, **(F)** Cas 9, (**G**) BAX and (**H**) Bcl-2 on Control, ISO and Rob pre-treated groups. Effects of Rob on ER-stress, apoptotic and survival related protein expression through western blot. **(I)** Western blot chemiluminescence of ERS related proteins. **(J)** Bip, **(K)** CHOP, and **(L)** PDI. (**M**) Western blot chemiluminescence of apoptosis related proteins. (**N**) Caspase 9. (**O**) Western blot chemiluminescence of survival related proteins. (**P**) AKT, (**Q**) GSK-3β and (**R**) ERK1/2. Equal protein loading was confirmed by β-actin. Densitometry was performed with the ImageJ software and densitometric analysis of the observed bands was intensity normalized to β-actin. *Denotes statistically significant differences in comparison with control: ns > 0.05, $^{*}p < 0.05$, $^{**}p < 0.01$, $^{***}p < 0.001$. #Denotes statistically significant differences in comparison with ISO group: $\#p < 0.05$, $\#\#p < 0.01$, $\#\#\#p < 0.001$. *In vitro* data are presented as mean ± SD of four independent experiments. *In vivo* data are presented as mean ± SD of six independent experiments. SD, standard deviation.

Data availability

The datasets used and/or analysed during the current study available from the corresponding author on reasonable request.

Received: 5 February 2025; Accepted: 11 September 2025
Published online: 15 October 2025

References

1. Tsao, C. W. et al. Heart disease and stroke statistics-2022 update: A report from the American heart association. *Circulation* **145**, e153–e639 (2022).
2. Borovac, J. A., D'Amario, D., Bozic, J. & Glavas, D. Sympathetic nervous system activation and heart failure: current state of evidence and the pathophysiology in the light of novel biomarkers. *World J. Cardiol.* **12**, 373–408 (2020).
3. Kalogeris, T., Baines, C. P., Krenz, M. & Korthuis, R. J. Cell biology of ischemia/reperfusion injury. In International Review of Cell and Molecular Biology Volume 298. pp. 229–317, Elsevier. (2012).
4. Janeesh, P. A., Sasikala, V., Dhanya, C. R. & Abraham, A. Robinin modulates TLR/NF-κB signaling pathway in oxidized LDL induced human peripheral blood mononuclear cells. *Int. Immunopharmacol.* **18**, 191–197 (2014).
5. Eichhorn, E. J. et al. Effect of Metoprolol on myocardial function and energetics in patients with nonischemic dilated cardiomyopathy: A randomized, double-blind, placebo-controlled study. *J. Am. Coll. Cardiol.* **24**, 1310–1320 (1994).
6. De Vereaux, P. J. et al. Effect of extended release metaprolol succinate in patients undergoing Non cardiac surgery: a randomized controlled trial. *Lancet. Vol* **371**, 1839–1847 (2008).
7. Kny, M. & Fielitz, J. Hidden agenda - the involvement of Endoplasmic reticulum stress and unfolded protein response in inflammation-induced muscle wasting. *Front. Immunol.* 13. (2022).
8. Quan, J. H. et al. VEGF production is regulated by the AKT/ERK1/2 signaling pathway and controls the proliferation of Toxoplasma gondii in ARPE-19 cells. Frontiers in cellular and infection microbiology 10. (2020).
9. Ménard, C. et al. Modulation of L-type calcium channel expression during retinoic acid-induced differentiation of H9C2 cardiac cells. *J. Biol. Chem.* **274**, 29063–29070 (1999).
10. Comelli, M. et al. Cardiac differentiation promotes mitochondria development and ameliorates oxidative capacity in H9c2 cardiomyoblasts. *Mitochondrion* **11**, 315–326 (2011).
11. Li, W. et al. Taurine attenuates isoproterenol-induced H9c2 cardiomyocytes hypertrophy by improving antioxidative ability and inhibiting calpain-1-mediated apoptosis. *Mol. Cell. Biochem.* **469**, 119–132 (2020).
12. Han, J. W., Kang, C., Kim, Y., Lee, M. G. & Kim, J. Y. Isoproterenol-induced hypertrophy of neonatal cardiac myocytes and H9c2 cell is dependent on TRPC3-regulated CaV1.2 expression. *Cell. Calcium.* **92**, 102305 (2020).
13. Karbassi, E. et al. Cardiomyocyte maturation: advances in knowledge and implications for regenerative medicine. *Nat. Rev. Cardiol.* **17**, 341–359 (2020).
14. Rona, G. Catecholamine cardiotoxicity. *J. Mol. Cell. Cardiol.* **17**, 291–306 (1985).
15. Singal, P. K., Beamish, R. E. & Dhalla, N. S. Potential oxidative pathways of catecholamines in the formation of lipid peroxides and genesis of heart disease. *Adv. Exp. Med. Biol.* **161**, 391–401 (1983).
16. Rajadurai, M. & Stanely Mainzen Prince, P. Preventive effect of naringin on lipid peroxides and antioxidants in isoproterenol-induced cardiotoxicity in Wistar rats: biochemical and histopathological evidences. *Toxicology* **228**, 259–268 (2006).
17. Radhakrishnan, A., Ensam, B., Moody, W. E. & Ludman, P. F. Isoprenaline induced myocardial infarction in a patient with high-grade atrioventricular block: a case report. *European heart journal.* (2023). Case reports 7.
18. Panda, S., Kar, A., Banerjee, T. & Sharma, N. Combined effects of Quercetin and Atenolol in reducing isoproterenol-induced cardiotoxicity in rats: possible mediation through scavenging free radicals. *Cardiovasc. Toxicol.* **12**, 235–242 (2012).
19. Patel, V., Upaganlawar, A., Zalawadia, R. & Balaraman, R. Cardioprotective effect of melatonin against isoproterenol induced myocardial infarction in rats: A biochemical, electrocardiographic and histoarchitectural evaluation. *Eur. J. Pharmacol.* **644**, 160–168 (2010).
20. Sabeena, F., Anandan, R., Kumar, S. H., Shiny, K. S. & Sankar, T. V. Effect of squalene on tissue defense system in isoproterenol-induced myocardial infarction in rats. *Pharmacol. Res.* **50**, 231–236 (2004).
21. Tappel, A. L. & Dillard, C. J. In vivo lipid peroxidation: measurement via exhaled pentane and protection by vitamin E. Federation proceedings 40, 174–178. (1981).
22. Wattanapitayakul, S. K. & Bauer, J. A. Oxidative pathways in cardiovascular disease: roles, mechanisms, and therapeutic implications. *Pharmacol. Ther.* **89**, 187–206 (2001).
23. Vanden Berghe, T., Kaiser, W. J., Bertrand, M. J. M. & Vandenabeele, P. Molecular crosstalk between apoptosis, necroptosis, and survival signaling. *Mol. Mol. Cell. Oncol.* **2, e975093.** (2015).
24. Obeidat, H. M. et al. Cardioprotective effect of taxifolin against isoproterenol-induced cardiac injury through decreasing oxidative stress, inflammation, and cell death, and activating Nrf2/HO-1 in mice. *Biomolecules* **12**, 1546 (2022).
25. Qian, S. et al. The role of BCL-2 family proteins in regulating apoptosis and cancer therapy. Frontiers in oncology 12. (2022).
26. Webster, K. A. Mitochondrial membrane permeabilization and cell death during myocardial infarction: roles of calcium and reactive oxygen species. *Future Cardiol.* **8**, 863–884 (2012).
27. Jensen, B. C., O'Connell, T. D. & Simpson, P. C. Alpha-1–adrenergic receptors in heart failure: the adaptive arm of the cardiac response to chronic catecholamine stimulation. *J. Cardiovasc. Pharmacol.* **63**, 291–301 (2014).

28. Fallah, A. et al. Therapeutic targeting of angiogenesis molecular pathways in angiogenesis-dependent diseases. *Biomed. Biomed. Pharmacother.* **110**, 775–785 (2019).
29. Narasimhan, B. et al. Therapeutic angiogenesis in coronary artery disease: a review of mechanisms and current approaches, expert Opin. *Expert Opin. Invest. Drugs*. **30**, 947–963 (2021).
30. Zhou, H., Li, X. M., Meinkoth, J. & Pittman, R. N. Akt regulates cell survival and apoptosis at a postmitochondrial level. *J. Cell Biol.* **151**, 483–494 (2000).

Author contributions
J.P.A. and A.N. conceptualized the study. A.N. conducted the literature review and data curation, and drafted the initial manuscript. J.P.A., A.V.A., and A.N. contributed to reviewing, editing, and finalizing the manuscript. All authors have reviewed and approved the final version of the work.

Funding
This research was supported by grants from the Department of Science and Technology under the Innovation in Science Pursuit of Inspired Research (INSPIRE) program, the Science and Engineering Research Board (SERB), India, the University Grants Commission (UGC), India, and the University of Kerala through Plan and Non-Plan funds.

Declarations

Competing interests
The authors declare no competing interests.

Ethics approval
All ethical guidelines were followed with the committee for the purpose of control and supervision of experiments on animals (CPCSEA), and ethical sanction no. IAEC 2-KU-01/2013-BCH-JA (08) for the conduct of animal experiments. This study was conducted in compliance with the ARRIVE guidelines.

Declaration of competing interests
The authors declare no competing interests related to the content of this article.

Additional information
Supplementary Information The online version contains supplementary material available at https://doi.org/10.1038/s41598-025-20063-0.

Correspondence and requests for materials should be addressed to J.P.A.

Reprints and permissions information is available at www.nature.com/reprints.

Publisher's note Springer Nature remains neutral with regard to jurisdictional claims in published maps and institutional affiliations.

Open Access This article is licensed under a Creative Commons Attribution-NonCommercial-NoDerivatives 4.0 International License, which permits any non-commercial use, sharing, distribution and reproduction in any medium or format, as long as you give appropriate credit to the original author(s) and the source, provide a link to the Creative Commons licence, and indicate if you modified the licensed material. You do not have permission under this licence to share adapted material derived from this article or parts of it. The images or other third party material in this article are included in the article's Creative Commons licence, unless indicated otherwise in a credit line to the material. If material is not included in the article's Creative Commons licence and your intended use is not permitted by statutory regulation or exceeds the permitted use, you will need to obtain permission directly from the copyright holder. To view a copy of this licence, visit http://creativecommons.org/licenses/by-nc-nd/4.0/.

© The Author(s) 2025